

MODELLING

Recent in-house developments in theoretical modelling of ultrasonic inspection

R K Chapman, J E Pearce, S F Burch, L Fradkin and M W Toft

Paper presented at NDT 2006, the 45th Annual British Conference on NDT, Stratford-upon-Avon, UK, September 2006.

Over the years British Energy, in collaboration with British Nuclear Group, has developed an extensive suite of computer codes for modelling the ultrasonic inspection of smooth and rough planar defects in ferritic steel components. The models are used to help in the design of new inspections, and to provide evidence on detection capability when writing a technical justification for inspection qualification purposes. This paper provides an update on the current status of these models, including their experimental validation. It also briefly describes some recent developments in modelling the scattering from rough defects, allowing for the effects of fine-scale roughness, and in modelling the inspection of surface-breaking cracks using the corner effect. In both cases, experimental validation plays an important role.

A recent application of the models, in the technical justification of an automated ultrasonic in-service inspection of a pressuriser weld at Sizewell B Power Station, is also described.

1. Introduction

Over the years British Energy, in collaboration with British Nuclear Group, has developed an extensive suite of computer codes for modelling the ultrasonic inspection of ferritic steel components. The models predict the echo amplitude, relative to a specified threshold level, as a probe scans over a component containing a hypothetical smooth or rough planar defect. The models are used to help in the design of new inspections, and to provide evidence on detection capability when writing a technical justification for inspection qualification purposes. Several papers give further information about the models, their experimental validation and some typical applications⁽¹⁾⁻⁽⁴⁾.

This paper starts with a brief overview of the current status of the models. Two recent developments of the models are then described: the effects of fine-scale roughness on the scattering from rough defects, and the use of ‘wedge’ diffraction coefficients to model the inspection of surface-breaking cracks using the corner effect. Finally, an outline is given of a recent typical application of the models, to the technical justification of an automated ultrasonic in-service inspection of a pressuriser weld at Sizewell B Power Station.

Robert K Chapman and John E Pearce are with British Energy Generation Ltd, Gloucester, GL4 3RS, UK. Tel: 01452 652179; Fax 01452 652699; E-mail: bob.chapman@british-energy.com

Stephen F Burch is with ESR Technology Ltd, Abingdon, OX14 4SA, UK.

Larissa Fradkin is with London South Bank University, London, SE1 0AA, UK.

Michael W Toft is a Consultant (Brookson Ltd), c/o British Energy address above.

2. Overview of current status of models

A list of the current in-house models for the ultrasonic inspection of ferritic steel components is given in Table 1. All these models are implemented as computer codes running on a PC. All the models predict the echo amplitudes from planar crack-like defects, and all except TRANGLE assume that the defect is smooth.

Table 1. In-house models for ultrasonic inspection of ferritic steel components

Code	Configuration	Scattering theory	Probe crystal	Focused probe?	Defect	Status
PEDGE	Direct pulse-echo	GTD	Single	No	Smooth	Released
PKIRCH	Direct pulse-echo	Kirchhoff	Single	No	Smooth	Released
TDPKIRCH	Direct pulse-echo (**)	Kirchhoff	Single	No	Smooth	Prototype
TRANGLE	Direct pulse-echo	Kirchhoff	Single	No	Rough	Prototype
TWINEDGE	Direct pulse-echo	GTD	Twin	No (*)	Smooth	Prototype
TWINKIRCH	Direct pulse-echo	Kirchhoff	Twin	No (*)	Smooth	Prototype
FOCUSEDGE	Direct pulse-echo	GTD	Single	Yes	Smooth	Prototype
FOCUSKIRCH	Direct pulse-echo	Kirchhoff	Single	Yes	Smooth	Prototype
COREEDGE	Corner effect	GTD	Single	No	Smooth	Prototype
CORKIRCH	Corner effect	Kirchhoff	Single	No	Smooth	Released
TEDGE	Tandem	GTD	Single	No	Smooth	Prototype
TKIRCH	Tandem	Kirchhoff	Single	No	Smooth	Prototype
TOFT	Time-of-flight diffraction	GTD	Single	No	Smooth	Prototype

(*) Other than focusing caused by toeing in of crystals
 (**) Time-dependent version of PKIRCH

The following parameters are specified by the user when running the models:

- Probe parameters, such as frequency, crystal size and pulse shape.
- Defect parameters, such as size, location, tilt and skew, together with surface morphology information if the defect is rough.
- Threshold parameters, such as size and depth of calibration reflector (side-drilled or flat-bottomed hole), threshold level relative to calibration reflector response and whether or not a DAC correction is applied.
- Scan limits and increments.
- Where relevant, additional parameters such as probe separation (for two-probe techniques) and component thickness.

Two different theories are used to model the scattering of the ultrasonic beam by the defect:

- The Geometrical Theory of Diffraction (GTD), which is a ray theory of diffraction which explicitly recognises the diffracted edge waves (‘tip diffraction’) by which smooth defects can be detected when misoriented to the incident ultrasonic beam. GTD generally works well but, in the form currently implemented in our models, it fails at the so-called caustics of the diffracted field, where neighbouring rays cross and infinite amplitudes are predicted. Recently, work has begun at London South Bank University to refine the GTD theory near caustics and overcome this problem.

□ Elastodynamic Kirchhoff theory, where the scattered field is computed by integrating over a series of secondary sources distributed over the surface of the defect. Kirchhoff theory is reasonably accurate for defects oriented in a direction favourable for detection by specular reflection, for example defects close to normal incidence for direct pulse-echo or near-vertical defects detected by the corner effect. At larger misorientations from specular, however, Kirchhoff theory becomes more inaccurate.

The two theories are largely complementary, in that caustics generally occur for near-specular conditions, so Kirchhoff theory can be used in cases where GTD breaks down.

The same probe beam model is used in all the codes for unfocused probes. This model has been verified against experiment⁽³⁾. The beam model used in the two codes for focused probes is a simple extension of the unfocused beam model, but this focused beam model has not yet been experimentally validated.

The final column of Table 1 shows the current status of the models. Some of the models have ‘released’ status, because they have been thoroughly validated against experiment and can be used with confidence within their regimes of validity for inspection design and capability assessment purposes. Other models have ‘prototype’ status because they have been less extensively validated, and are more suitable for use in a supporting role.

3. Two recent developments

3.1 Fine-scale roughness corrections to rough defect model TRANGLE

The model TRANGLE predicts the ultrasonic echoes from a rough planar crack in ferritic steel when inspected with a pulse-echo probe. The crack is represented as a fine mosaic of interlocking triangular facets (Figure 1). The scattering from each facet is calculated using the Kirchhoff theory approximation, assuming the facet itself to be smooth. The total echo is then obtained by summing the responses from each facet.

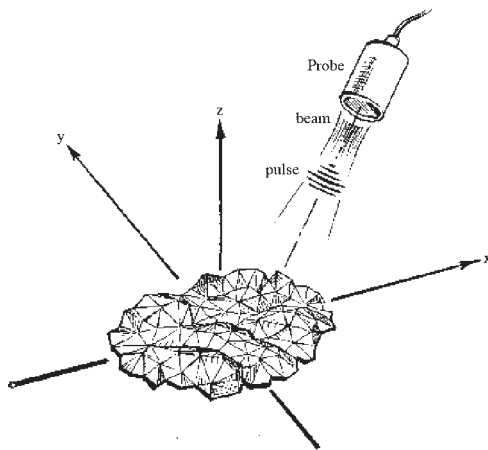


Figure 1. Schematic diagram of configuration modelled by TRANGLE

Experimental validation studies of this model have been undertaken⁽⁴⁾, using three embedded rough defects in test blocks, and seven contact probes with different beam angles to obtain seven different angles of incidence on the defects between 0 and 30°. These studies showed the performance of TRANGLE to be encouraging, but with a systematic over-prediction of defect response, by up to around 4 dB, for angles of incidence below about 20°. At higher angles of incidence, the model predictions were generally pessimistic, again by up to around 4 dB, although under-prediction of defect response is of less concern when applying the models to practical inspection situations.

It was thought that the over-prediction of response for small angles of incidence might be due to the neglect of fine-scale roughness when calculating the response of each individual triangular facet. Various methods of correcting for this fine-scale roughness have recently been investigated, all based on applying an exponential attenuation factor α of the form:

$$\alpha = \exp(-2\sigma^2 k^2 \cos^2 \theta) \dots\dots\dots(1)$$

where σ is the root-mean-square fine-scale roughness, k is the wavenumber and θ is the angle of incidence of the beam. This factor⁽⁵⁾ is a result of applying Kirchhoff theory to a rough surface with a Gaussian height distribution, and applies to the coherent (specularly reflected) field. Three ways of applying this factor were investigated:

- (a) facet by facet to all the facets, where θ is the local angle of incidence on the individual facet;
- (b) as in (a), but only to facets oriented within a certain angle of normal incidence (on the grounds that the factor only applies to the specularly reflected field);
- (c) globally to the whole defect response, where θ is now the angle of incidence on the mean plane of the defect.

Method (c) was found to be the most successful in practice for the three defects in the experimental study, as well as being the simplest to apply. Figure 2 shows the TRANGLE predictions both before and after correction for fine-scale roughness using this method, compared with the experimental data. For each probe angle, the plots show the 50th percentile of the response as the probe scans, *ie* the median response level for probe positions lying within the analysis area. This area was based on the 6 dB-down contour of the measured defect response, where the contour was calculated relative to the nearest local maximum.

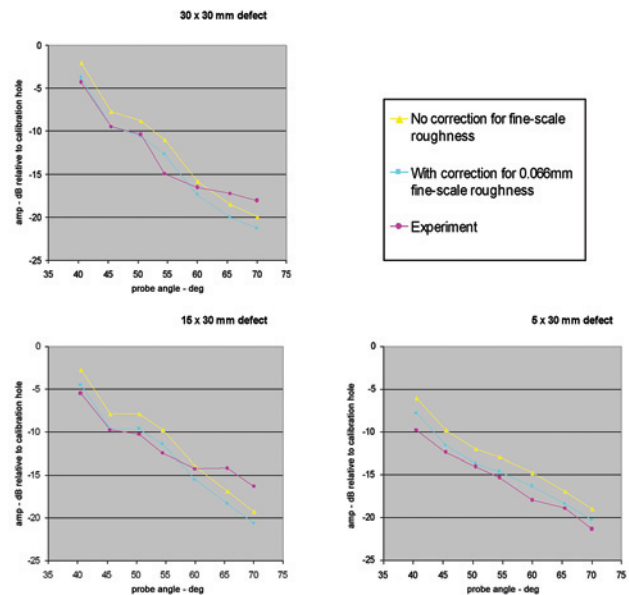


Figure 2. Pulse-echo responses from three different rough defects with 7 different probe beam angles: comparison between experiment and globally corrected TRANGLE code predictions. All three defects are tilted by 50°, so the 40° probe gives normal incidence on the defects

The global correction for the effects of fine-scale roughness reduces the over-prediction of the model near normal incidence to a maximum of about 2.2 dB. Under-predictions of up to about 4.3 dB are generally observed at higher angles of incidence, but these are of less concern since the model predictions are then pessimistic.

The value of fine-scale roughness chosen here (σ in equation (1) above) was 0.066 mm. This value was chosen empirically to give exact agreement with experiment for one particular case (30 x 30 mm

defect, 45° probe – ie 5° off normal incidence), and is about one-third of the roughness of the whole defect (0.20 mm), as measured by a custom-built roughness-measuring machine⁽⁴⁾. Further work is needed to decide which value of fine-scale roughness to use in a case where experimental data is not available.

3.2 Diffraction coefficients for surface-breaking cracks

One of the in-house models, COREEDGE, uses GTD to model the pulse-echo inspection of a smooth planar defect at or near the back-wall of the component using the ‘corner effect’ mechanism. This corner effect is optimised when the defect is vertical, because a specular ‘cat’s-eye’ reflection is then obtained. However, the defect may still be detectable if it is tilted, through diffracted edge waves from the crack tips. If the defect breaks the back-wall, one of these edge waves comes from the corner or ‘wedge’ formed between the defect and the back-wall (Figure 3).

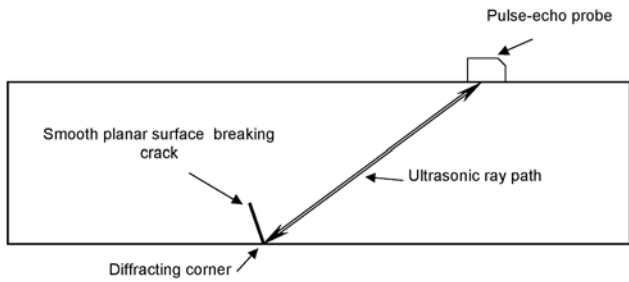


Figure 3. Diffraction from a corner for surface-breaking cracks

In order to model this configuration using GTD, it is necessary to know the diffraction coefficients for this elastic wedge configuration. For horizontally polarised shear (SH) waves, this is an acoustic problem for which an analytic solution has long been available⁽⁶⁾. For compression waves and vertically polarised shear (SV) waves, the problem is elastic and is much more difficult to solve. Recently, however, workers at London South Bank University (LSBU) have solved this problem using an approach which leads to singular integral equations which are then solved numerically⁽⁷⁾. The LSBU computer codes can be run to generate look-up tables of the wedge diffraction coefficients, which can then be read by COREEDGE in order to predict echo amplitudes from surface-breaking cracks.

In order to validate the LSBU work experimentally, measurements have been made of the back-scatter from the vertex of a wedge of ferritic steel with an angle of 100° (Figure 4), using 0° compression or shear wave probes. For compression waves, the experimental results for the amplitudes and phases of the diffraction coefficients are compared with the LSBU theoretical solution in Figures 5 and 6. It can be seen that the agreement is good. Similar levels of agreement are obtained for horizontally

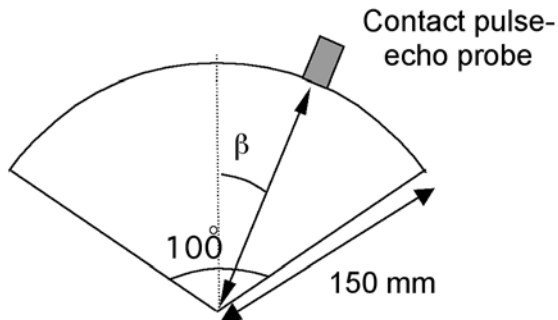


Figure 4. Experimental set-up for measuring wedge diffraction coefficients. β is the angle to the wedge bisector and is the angle plotted on the horizontal axes of Figures 5 and 6 below

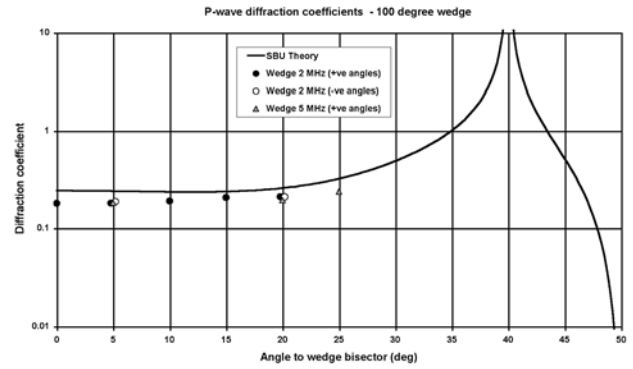


Figure 5. Amplitudes of back-scattered wedge diffraction coefficients for compression waves in a 100° vertex: comparison between experiment (plotted points) and LSBU theory (solid curve)

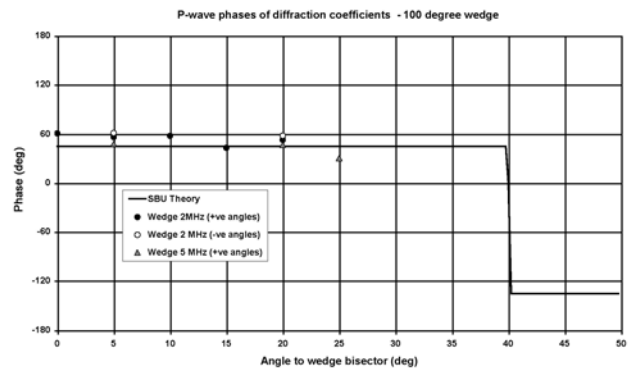


Figure 6. Phases of back-scattered wedge diffraction coefficients for compression waves in a 100° vertex: comparison between experiment (plotted points) and LSBU theory (solid curve)

polarised shear (SH) waves using the analytic theoretical solution⁽⁷⁾, and for vertically polarised shear (SV) waves using the LSBU theory, though the latter is complicated by the rapid variation in the theoretical diffraction coefficient for angles of incidence near the critical angle (about 7° from the wedge bisector). Similar rapid variations occur near the critical angle in the case of diffraction from an embedded crack tip⁽¹⁾.

4. Application of modelling to Sizewell B pressuriser inspection

As an illustration of how the models are used in practice, we now describe a recent application to an in-service automated ultrasonic inspection of the pressuriser upper head-to-shell weld at Sizewell B Power Station. This weld connects the upper cylindrical shell section of the pressuriser to the hemispherical head: it is about 2350 mm in diameter and 115 mm thick, made of ferritic steel with ~8 mm stainless steel cladding on the inside surface. This weld had previously been inspected in-service during the 2003 outage, but the inspection was restricted to about 75% of the circumference due to the presence of support lugs and other steelwork which restricted the movement of the scanner. A new scanner was designed and procured, and a new inspection procedure raised, in order to overcome these restrictions. The new inspection, which was applied during the 2005 outage, needed to have a highly reliable, qualified detection capability. The inspection was therefore qualified according to the methodology of ENIQ (the European Network for Inspection and Qualification). This involved the production of a Technical Justification giving evidence on the capability of the inspection procedure, as well as test-piece trials, including blind trials of the inspection personnel (data interpreters). Modelling was used as one of the sources of evidence in the technical justification.

The defect detection requirements covered both smooth and rough defects, and both longitudinal and transverse defects. For simplicity we concentrate here on the modelling work done for the smooth longitudinal defects. The key requirement is for reliable detection of planar defects of size 30 mm long by 15 mm through-wall (the 'qualification size'), with a ligament to either the inner or outer surface of up to 5 mm and a tilt/skew orientation within 10° of the through-wall direction.

The scans prescribed in the procedure are shown in Figures 7 and 8 – these include both half- and full-skip scans from both sides of the weld, though the support lugs do restrict the scanning extents for the 'up' scans, even with the redesigned scanner (Figure 9). Access is only available from the outside surface of the pressuriser as shown.

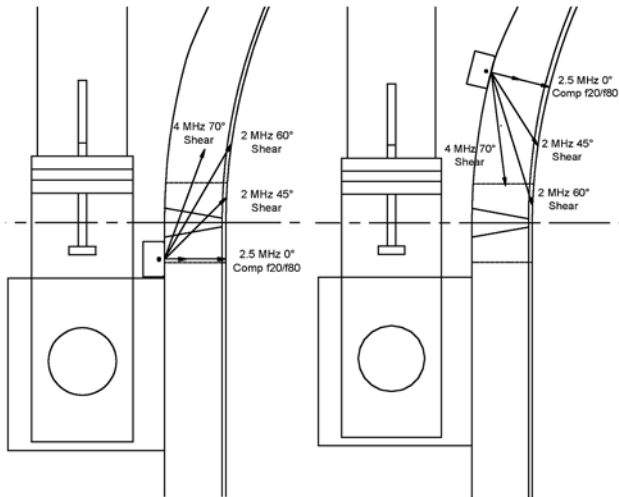


Figure 7. Scan design for Sizewell B pressuriser weld inspection: half-skip up scans (left) and half-skip down scans (right)

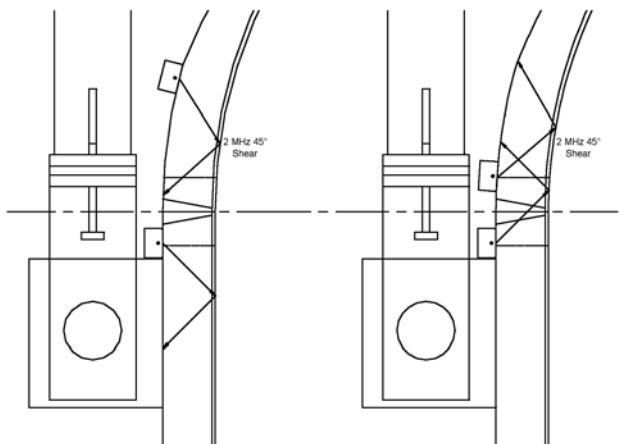


Figure 8. Scan design for Sizewell B pressuriser weld inspection: full-skip down scans (left) and full-skip up scans (right)

The modelling approach adopted was to select qualification size defects of various tilts and skews, either surface-breaking to the inner or outer surfaces or having a 5 mm ligament. The responses of the various probes when inspecting these hypothetical defects was then determined theoretically using PEDGE for direct pulse-echo responses and CORKIRCH for corner effect responses. Examples of the predictions are shown in Table 2. The outcome of this modelling was that all the modelled smooth defects within the defect description (unshaded responses) were predicted to be detectable above the reporting threshold. This remains true even where scanning restrictions apply and we pessimistically assume that we have to rely on the down scans only.

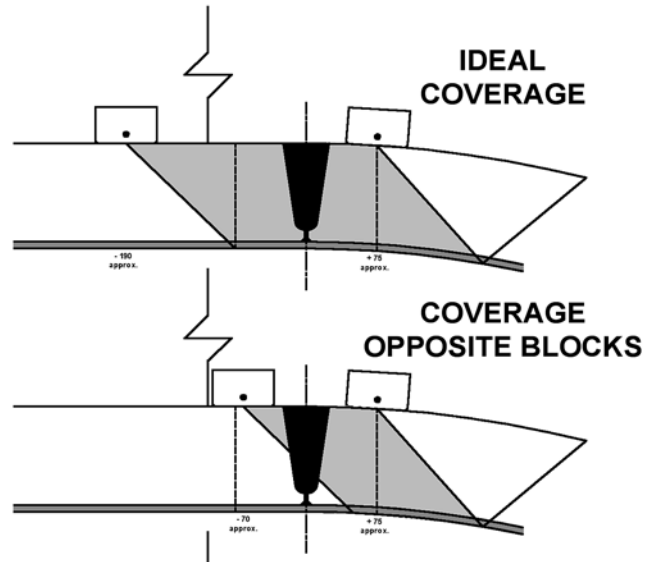


Figure 9. Example of scan restriction due to support lugs: 45° probe up scan to half skip

Table 2. Predicted responses from smooth surface-breaking 30 x 15 mm semi-circular defects at outer surface. Amplitudes are in dB relative to the reporting threshold. The overall best scans for each defect are highlighted in red. The shaded responses are for defects outside the defect description but included to give a fuller picture of the inspection capability

Defect tilt (deg)	Defect skew (deg)	Best up scan		Best down scan		Other modelled scans predicting detection	
		dB	Scan	dB	Scan	dB	Scan
0	0	+43	45° fs c U	+43	45° fs c D	+14 +15	70° d U 70° d D
10	0	+18	70° d U	+22	45° fs c D	+17 +7	45° fs c U 70° d D
-10	0	+22	45° fs c U	+18	70° d D	+6 +17	70° d U 45° fs c D
0	3	+32	45° fs c U	+32	45° fs c D		
10	3	+11	45° fs c U	+17	45° fs c D		
-10	3	+17	45° fs c U	+11	45° fs c D		
0	5	+21	45° fs c U	+21	45° fs c D		
10	5	+14	45° fs c U	+8	45° fs c D		
-10	5	+8	45° fs c U	+14	45° fs c D		
0	7	+12	45° fs c U	+12	45° fs c D		
10	7	+12	45° fs c U	+5	45° fs c D		
-10	7	+5	45° fs c U	+12	45° fs c D		
0	10	+7	45° fs c U	+7	45° fs c D		
10	10	+7	45° fs c U	0	45° fs c D		
-10	10	0	45° fs c U	+7	45° fs c D		

Key: fs = full skip; c = corner effect; d = direct pulse-echo; U = up scan; D = down scan

It should be emphasised that modelling was only one source of evidence within the technical justification – this is typical of how modelling is used as part of a multi-legged argument. In this case, other sources of evidence included in the technical justification included:

- ❑ Physical reasoning and coverage diagrams.
- ❑ Identification of parameters which could affect performance and arguments to show that these would be adequately controlled.
- ❑ Equipment functional checks (hardware and software).
- ❑ Experience, training and qualification of personnel.
- ❑ Previous experience of the flaw detector, motor controllers, data collection software and data analysis software in qualified inspections.

- Practical evidence from validated inspections on similar components and welds.
- Practical evidence from commissioning of the equipment and procedure on a full-scale mock-up.

5. Conclusions

This paper has summarised the current status of the in-house theoretical models of ultrasonic inspection available within British Energy. Two recent examples of development work have been described, both involving comparisons with experimental validation results. A recent typical application of the models, to an automated inspection of a Sizewell B pressuriser weld, has been outlined.

Acknowledgements

This paper is published by permission of British Energy Generation Ltd.

References

1. R K Chapman, 'A system model for the ultrasonic inspection of smooth planar cracks', *J NDE*, 9, pp 197-210, 1990.
2. R K Chapman and M W Toft, 'Theoretical prediction and experimental verification of time-dependent ultrasonic responses of smooth defects'. In *Proc 4th European Conf on Non-Destructive Testing*, London, Sept 1987, ed J M Farley and R W Nichols, Vol 1, pp 684-694, 1988.
3. S F Burch, N J Collett and A P Wein, 'Experimental verification of CEGB theoretical models for ultrasonic inspection'. In *Proc 1988 Annual Conference of British Institute of NDT*, Portsmouth, pp 405-423, Sept 1988.
4. S F Burch, N Collett, R K Chapman and M W Toft, 'Experimental validation of the TRANGLE and related NDT codes for modelling the ultrasonic inspection of rough cracks', *Insight*, 46, pp 74-76, 2004.
5. C Eckart, 'The scattering of sound from the sea surface', *J Acoust Soc Amer*, 25, pp 556-570, 1953.
6. D S Jones, 'The theory of electromagnetism', pp 608-612, Pergamon Press, Oxford, 1964.
7. V Kamotski, B A Samokish, L Fradkin, V M Babich and V A Borovikov, 'On Budaev and Bogy's approach to diffraction by a 2D traction-free elastic wedge'. To appear in *SIAM J Appl Math*.